Soft Matter

Charge polarization near dielectric interfaces and the multiple-scattering formalism

Journal:	*Soft Matter*
Manuscript ID	SM-REV-10-2018-002196.R2
Article Type:	Review Article
Date Submitted by the Author:	02-Feb-2019
Complete List of Authors:	Qin, Jian; Stanford University, Chemical Engineering

Soft Matter

ARTICLE TYPE

Cite this: DOI: 10.1039/xxxxxxxxxx

Charge polarization near dielectric interfaces and the multiple-scattering formalism

Jian Qin[a]

Received Date
Accepted Date

DOI: 10.1039/xxxxxxxxxx

www.rsc.org/journalname

Interfacial charge polarization is ubiquitous in systems with sharp dielectric contrast. Fully resolving the interfacial charges often relies on demanding numerical algorithms to solve the boundary value problem. The recent development of an analytical multiple-scattering formalism to solve the interfacial charge polarization problem for particles carrying monopolar, dipolar, and multipolar charges is reviewed. Every term produced in this formalism has a simple interpretation, and terms for spherical particles can be rapidly evaluated using an image-line construction. Several practical applications of this formalism are illustrated. A dielectric virial expansion for polarizable particles based on this formalism is also described. The origins of singular polarization charges for particles in close contact are explained and evaluated for both dielectric and conducting spheres.

Applying an electrical field to dielectric materials perturbs their charge distribution and results in a net polarization that quantifies the degree of spatial charge separation.[1] For weak fields, the polarization grows linearly with field strength and is governed by the dielectric permittivity tensor, which reduces to a scalar constant in isotropic dielectrics. The relative dielectric permittivity spans a wide numerical range of values:[2] it is unity for vacuum, about 80 for water at room temperature, between 2 and 10 for most organics, and, for many oxides, falls between 15 and 40.

Interfacial polarization is a unique phenomenon which occurs near the interfaces between materials with distinct dielectric permittivities. The bulk material on each side of the interface responds to externally applied fields differently, causing different degrees of polarization which do not compensate each other resulting in a net surface charge. These net charges at the interface have been extensively investigated over the past few decades, and remain an attractive topic owing both to practical concerns and fundamental interests. For example, these bound charges are relevant in various applications, including the movement of ions through nanochannels in fuel cells[3] and cell membranes,[4] self-assembly of charged particles,[5] aggregation of granular materials,[6,7] and stability of emulsions and colloidal solutions.[8–10] On the other hand, they are also pertinent to fundamental studies of electrolyte solutions, such as determining the density profile[11,12] and mobility[13] of ions near dielectric interfaces, the variation of dielectric constant in continuum theories[14,15] and the surface tension of ionic solutions.[16]

In particular, the surface tension of electrolyte solutions has attracted significant attention due to its potential relevance to the Hofmeister effect, and its great importance in biology.[17] Unlike surfactant solutions, the surface tension of aqueous solutions has been found to exhibit non-trivial dependence on the concentration of electrolytes. Langmuir[18] considered Gibbs adsorption isotherms, and postulated that the initial increase of surface tension with electrolyte concentration results from ions depletion near the air-water interface. Wagner,[19] and Onsager and Samaras[16] applied the Debye-Hückel theory to account for the depletion of ions by repulsive ion-image interactions at the air-water interface. These theories do not explicitly account for specificities of the ions, such as ion size and polarizability, and fail to explain the Hofmeister effect.[20] Recent evidence from both simulation[21] and experiment[22] has suggested that, in some cases, there is an enhanced concentration of anions near the interface. A modified Poisson-Boltzmann theory was applied to account for the effects of ion size and polarizability.[23,24] These developments have provided compelling arguments for incorporating the polarization of ions and interfaces into more realistic treatments of ionic solutions.

In particulate aggregates, one particularly intriguing phenomenon has been often described as polarization-induced like-charge attraction.[25–27] Depending on the ratio of net charges carried by particles, and the ratio of dielectric permittivities between the particles and the medium, it has been found that the normally repulsive potential between like-charged particles may become attractive at small inter-particle separation. This essentially arises due to boundary effects, and analogous phenomena have been observed in colloidal particles near reflective walls.[28] Similar effects in many-body particle aggregates may manifest as

[a] Department of Chemical Engineering, Stanford University, Stanford 94305, USA. Tel: 01-650-724-7644; Email: jianq@stanford.edu

non-additive inter-particle potentials, as was demonstrated experimentally in colloidal particles.[29,30] The impact of such strong polarization on the cohesive energy of the self-assembled periodic aggregates of polarizable charged colloidal or granular particles has also been suggested (**Fig. 2**).[27]

In order to efficiently quantify the strength of interfacial charge polarization, many theoretical and numerical approaches have been developed. For systems involving sharp dielectric interfaces, an induced surface charge density is frequently introduced to account for the sharp boundary discontinuity.[31–34] For systems involving smoothly varying dielectric permittivities, variational methods have been developed.[35] We focus in this work on systems involving sharp dielectric discontinuities, for which the strength of interfacial polarization is controlled by the relative 'jump' in permittivity at the interface (see Eq. (1) below).

We will review and summarize an analytical, multiple-scattering formalism developed to resolve the interfacial charge polarization.[36–38] In such a formalism, the electrostatic boundary value problem of many-body particulate systems is solved iteratively, which yields a series expansion for the system energy expressed solely in terms of particle positions. Applying this formalism to solve practical problems requires the Green's function of the single particles to be known *a priori*, which can be analytically resolved only for simple geometries, otherwise requiring numerical tabulations. For spherical particles, it has been found that the Green's function can be rapidly evaluated by an image-line construction, which was first discovered by Neumann,[39] and then repeatedly discovered in varying contexts.[33,36,40–42]

In the following, the latest results obtained from the application of the multiple-scattering theory combined with the image charges applied to aggregates of spherical particles will be presented. The model, notation, and structure of the multiple-scattering formalism will be explained in the next section, which covers systems with monopolar charges, multipolar charges, and the application of external fields. Subsequently, the application of the theory for evaluating the energy of aggregates and for studying the cohesive energy of colloidal lattices with polarization contributions will be described, and a dielectric virial expansion for the static dielectric permittivity will be presented. In these examples, the effects of polarization have revealed themselves in unexpected ways. The polarization, however, becomes strongest when particles form close contact or for conducting particles whose static dielectric permittivity can be treated as infinite. We shall review the nature of contact singularity and show how it can be isolated and combined with numerical approaches to generate finite results on the cohesive energy of clusters of conducting particles in close contact. A judicious list of unresolved problems and possible future directions will be noted in the last section.

1 Energy of polarizable particles

A generic model system is a composite of inclusions embedded into a dielectrically continuous medium, such as a polymer. The medium's static dielectric permittivity is denoted ϵ_{out}. The inclusions may have arbitrary shape, and may be polydisperse. Indexing the inclusions by i, we may denote their static dielectric permittivity by $\epsilon_{\text{in},i}$. For notational simplicity, however, we will drop the reference to particle index, and denote the internal permittivity by ϵ_{in}. The generalization of the multiple-scattering treatment to heterogeneous dielectric particles is straightforward. A set of free charges indexed by α are distributed in the system, and are parameterized by position $\boldsymbol{R}_\alpha$ and charge Q_α.

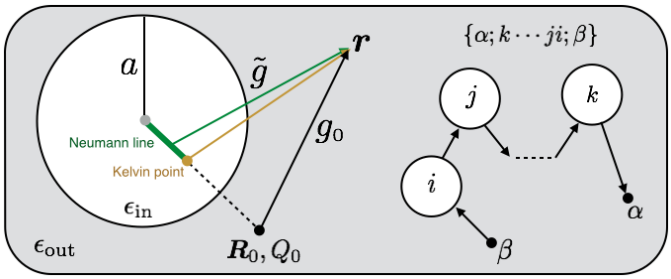

Fig. 1 Interfacial polarization mediated by a single and multiple interfaces. The direct static field produced by the source charge Q_0 placed at $\boldsymbol{R}_0$ is $g_0 = \frac{Q_0}{4\pi\epsilon_0\epsilon_{\text{out}}|\boldsymbol{r}-\boldsymbol{R}_0|}$. The indirect contribution from a single polarized surface is denoted by the one-particle Green's function $\tilde{g}$, which can be effectively represented by the total contributions from the Kelvin image point (orange) and the Neumann image line (green). The exact form of $\tilde{g}$ is given as Eq. (23). The polarization involving multiple interfaces, denoted using the string notation by $\{\alpha; k \cdots ji; \beta\}$, is illustrated in the right. Distance of the Kelvin point to the origin is a^2/R_0, where R_0 is the distance of the source charge to the center of sphere. The Neumann image line connects the origin of the sphere to the Kelvin image point.

The basic question is to find the electrostatic potential for a given charge distribution. In the absence of a dielectric interface, the charge distribution is given by Coulomb's law. In the presence of interfacial polarization, in general no simple, closed-form solution is possible. A few known results are discussed in sec. 3.

The multiple-scattering formalism[27,36] aims to solve for the potential iteratively, by considering chains of interfacial polarization with increasing complexity. This approach is generic, and applies to most linear systems with sharp boundaries. For instance, the viscosity of suspensions[43] in the low-Reynolds number regime[44] is a closely analogous problem.

1.1 Boundary condition

The primary task is to solve Poisson's equation, for given free charge distribution $\rho(\boldsymbol{r})$, with spatially varying dielectric permittivity, $\nabla\cdot\epsilon(\boldsymbol{r})\nabla\phi(\boldsymbol{r}) = -\rho(\boldsymbol{r})$ subject to the boundary condition governed by Gauss's law, where the dielectric permittivity $\epsilon(\boldsymbol{r})$ is a constant ϵ_{out} outside, and ϵ_{in} inside the particles. The electrostatic potential $\phi(\boldsymbol{r})$ and the tangential component of the field $\boldsymbol{E}(\boldsymbol{r}) \equiv -\nabla\phi(\boldsymbol{r})$ are continuous at the interface. The normal component of the field is discontinuous, and is governed by the relative values of the permittivity on the two sides of the interface. In the absence of the free surface charge, the boundary condition is

$$\epsilon_{\text{in}}\boldsymbol{E}_{\text{in}}\cdot\hat{\boldsymbol{n}} = \epsilon_{\text{out}}\boldsymbol{E}_{\text{out}}\cdot\hat{\boldsymbol{n}}, \tag{1}$$

where $\hat{\boldsymbol{n}}$ is the normal to the interface.

The potential generated by a single point source Q_0 at position

$\boldsymbol{R}_0$ near a particle inclusion can be written symbolically as

$$\phi(\boldsymbol{r}) = g_i(\boldsymbol{r};\boldsymbol{R}_0,Q_0), \tag{2}$$

where g_i is the Green's function for the boundary of the particle with index i. In the absence of the boundary, the Green's function reads

$$g_0(\boldsymbol{r};\boldsymbol{R}_0,Q_0) = \frac{Q_0}{4\pi\epsilon_0\epsilon_{\text{out}}|\boldsymbol{r}-\boldsymbol{R}_0|}. \tag{3}$$

In the presence of the boundary, the Green's function can be written as a sum of contributions from the free charge and that from the induced, bound surface charges, i.e.,

$$g_i(\boldsymbol{r};\boldsymbol{R}_0,Q_0) = g_0(\boldsymbol{r};\boldsymbol{R}_0,Q_0) + \frac{1}{4\pi\epsilon_0\epsilon_{\text{out}}}\int_{\partial\Omega_i} \mathrm{d}s\, \frac{\sigma(\boldsymbol{s})}{|\boldsymbol{r}-\boldsymbol{r}(\boldsymbol{s})|}. \tag{4}$$

Above, ϵ_0 is the vacuum permittivity, $\mathrm{d}\boldsymbol{s}$ is the surface element on the boundary $\partial\Omega_i$, $\sigma(\boldsymbol{s})$ is the surface charge density induced by free charge Q_0 placed at $\boldsymbol{R}_0$, and $\boldsymbol{r}(\boldsymbol{s})$ is the spatial coordinate of the element $\boldsymbol{s}$. The position of source charge $\boldsymbol{R}_i$ is assumed to be outside the inclusion; the opposite case can be treated nearly identically.[33,36]

Since the first term in Eq. (4) is smooth everywhere except at the source, in order to match the boundary condition Eq. (1) the surface charge density has to be introduced and adjusted according to the source position $\boldsymbol{R}_0$. In typical numerical approaches, the surface charge density is discretized, and is used to convert Eq. (1) into a vector identity, the number of entries in the vector being the same as the number of surface elements,[31,32] or and the number of basis modes used.[25,26,45] Inverting the linear system gives the surface charge density. Alternatively, the following will show that the surface charge can be formally and iteratively solved by using a *multiple-scattering* formalism.

1.2 Multiple-scattering for a point source

Consider first how the interface is polarized by the free charge Q_0 at $\boldsymbol{R}_0$. The zeroth order field is given by the potential $\phi_0(\boldsymbol{r}) = g_0(\boldsymbol{r};\boldsymbol{R}_0,Q_0)$ and the electric field is $\boldsymbol{E}_0 = -\nabla\phi_0$. The induced surface charge density at this order is given by $\sigma_0 = (\epsilon_{\text{in}}-\epsilon_{\text{out}})\boldsymbol{E}_0\cdot\hat{\boldsymbol{n}}$. The potential generated by this surface charge

$$\phi_1(\boldsymbol{r}) = \frac{1}{4\pi\epsilon_0\epsilon_{\text{out}}}\int_{\partial\Omega_i} \mathrm{d}s\, \frac{\sigma_0(\boldsymbol{s})}{|\boldsymbol{r}-\boldsymbol{r}(\boldsymbol{s})|} \tag{5}$$

produces the additional field $\boldsymbol{E}_1 = -\nabla\phi_1(\boldsymbol{r})$. The field $\boldsymbol{E}_1$ induces the next order of polarization charge $\sigma_1 = \epsilon_0(\epsilon_{\text{in}}-\epsilon_{\text{out}})\boldsymbol{E}_1\cdot\hat{\boldsymbol{n}}$, where the normal $\hat{\boldsymbol{n}}$ relates to the surface element by $\hat{\boldsymbol{n}} = \mathrm{d}\boldsymbol{s}/\mathrm{d}s$. In terms of potential ϕ_1, the surface charge can be equivalently written as $\sigma_1 = -\epsilon_0(\epsilon_{\text{in}}-\epsilon_{\text{out}})\nabla_{\hat{\boldsymbol{n}}}\phi_1(\boldsymbol{r})$. This procedure may continue iteratively, up to infinite number of polarizations, i.e. by *scattering*.

The resulting surface charge density, which satisfies the boundary condition and is needed by Eq. (4), is the sum

$$\sigma = \sigma_0 + \sigma_1 + \cdots \tag{6}$$

Note that the $(n+1)$th order surface charge density σ_{n+1} is uniquely determined by the term from the previous order of scattering σ_n, which is ultimately traced back to σ_0. As a result, the total charge density is uniquely determined by the source, $\boldsymbol{R}_0$ and Q_0. Formally, we may write Eq. (4), the potential generated by the source and the polarized interface $\partial\Omega_i$ as

$$g_i(\boldsymbol{r};\boldsymbol{R}_0,Q_0) = g_0(\boldsymbol{r};\boldsymbol{R}_0,Q_0) + \tilde{g}_i(\boldsymbol{r};\boldsymbol{R}_0,Q_0), \tag{7}$$

the second term $\tilde{g}_i$ reflecting the contributions from induced surface charges, whose exact expression will be provided in sec. 3 (Eq. (23)). Since Poisson's equation is linear, the potential generated by an ensemble of charges near a single interface is the superposition of individual contributions.

When multiple interfaces are present, every interface is not only polarized by the source charge, but also by the induced surface charges from *all* the other interfaces. The complete potential should include contributions from an arbitrary number of surfaces, and from arbitrary scattering trajectories. The contributions from one source term and the multiple, primary surface scattering is given by

$$g_0(\boldsymbol{r};\boldsymbol{R}_0,Q_0) + \sum_i \tilde{g}_i(\boldsymbol{r};\boldsymbol{R}_0,Q_0), \tag{8}$$

in which the summation is over all the interfaces. The contribution from the secondary surface scattering is given by

$$\sum_{j,j\neq i}\sum_i \tilde{g}_j\circ\tilde{g}_i(\boldsymbol{r}(\boldsymbol{s}_j);\boldsymbol{R}_0,Q_0). \tag{9}$$

Here, $\boldsymbol{r}(\boldsymbol{s}_j)$ is the spatial coordinate of the surface element on the j-th surface. By the nature of consecutive scattering, j has to be distinct from i. The operator '$\circ$' implies the integration over the surface charges on the jth surface induced by those on the surface i. The exact expression for the composite Green's function $\tilde{g}_j\circ\tilde{g}_i$ will be given in sec. 3 (Eq. (25)) after the exact form of the single surface Green's function $\tilde{g}$, Eq. (23), is introduced. The current section is focused on the structure of the multiple-scattering formalism, so the algebraic details is deliberately avoided. To simplify the notation, we write the above in terms of the *string* notation, as follows

$$\sum_{j,j\neq i}\sum_i \{\boldsymbol{r};ji;0\}. \tag{10}$$

The implication of the above is identical to Eq. (9). Similarly, the tertiary contribution to potential can be written

$$\sum_{k,k\neq j}\sum_{j,j\neq i}\sum_i \{\boldsymbol{r};kji;0\}. \tag{11}$$

The higher order terms can be constructed by analogy. The total potential at position $\boldsymbol{r}$ generated by the source charge and by all the polarized surfaces is obtained by collecting contributions from all orders of surface scattering, i.e.,

$$\phi(\boldsymbol{r};\boldsymbol{R}_0,Q_0) = \{\boldsymbol{r};0\} + \sum_i \{\boldsymbol{r};i;0\} + \sum_{j,j\neq i}\sum_i \{\boldsymbol{r};ji;0\} + \sum_{k,k\neq j}\sum_{j,j\neq i}\sum_i \{\boldsymbol{r};kji;0\} + \cdots \tag{12}$$

This series expansion formally solves the boundary value problem for the potential generated by one point source, the essence of which is to express the total Green's function using those of individual surfaces.

1.3 Polarization energy

The potentials produced by different point charges are additive. For an ensemble of charges, the total potential at position $\boldsymbol{r}$ is simply the summation of terms similar to Eq. (12) due to all the charges. The total energy is the summation of products between all the free charges and the potential evaluated on them. For concreteness, we denote the free charges by α, β, etc. The total energy can thus be written

$$E = \frac{1}{2}\sum_{\alpha} Q_\alpha \sum_{\beta} \phi(\boldsymbol{R}_\alpha; \boldsymbol{R}_\beta, Q_\beta) \tag{13}$$

The ranges of both α and β are not restricted. The factor $1/2$ accounts for the over-counting in the pair-wise interaction between dissimilar charges.

By using the explicit expansion of the potential from single charges, Eq. (12), the total energy can be ordered by the number of surface scatterings involved. We may write

$$E = E_1 + E_2 + E_3 + E_4 \cdots \tag{14}$$

Above, E_1 and E_2 etc. represent the one-body, two-body energies that involve no surface scattering. The higher order terms E_n, with $n \geq 3$, involve $n-2$ surface scatterings.

The string notation for electrostatic potential evaluated at the position $\boldsymbol{r}$ introduced above can be generalized to evaluate the energy. For instance, the typical term in the summation, Eq. (13), $Q_\alpha \phi(\boldsymbol{R}_\alpha; \boldsymbol{R}_\beta, Q_\beta)$, may be written for brevity as

$$\{\alpha;\beta\} + \sum_i \{\alpha;i;\beta\} + \sum_j \sum_i \{\alpha;ji;\beta\} + \cdots \tag{15}$$

where the electrostatic potentially is naturally evaluated at the position $\boldsymbol{R}_\alpha$. The above expressions include all types of interactions between charges α and β mediated by an arbitrary combination of intermediate surface polarizations indexed with i, j etc. In terms of the string notation introduced above, these terms are transparently given by:

$$\begin{aligned} E_1 &= \frac{1}{2}\sum_{\alpha} \{\alpha;\alpha\} \\ E_2 &= \frac{1}{2}\sum_{\alpha}\sum_{\beta} \{\alpha;\beta\} \\ E_3 &= \frac{1}{2}\sum_{\alpha}\sum_{i}\sum_{\beta} \{\alpha;i;\beta\} \\ E_4 &= \frac{1}{2}\sum_{\alpha}\sum_{j}\sum_{i}\sum_{\beta} \{\alpha;ji;\beta\} \\ &\cdots \end{aligned} \tag{16}$$

Note that the neighboring indices are implicitly assumed to be different. The term E_1 can be interpreted as the minimum order of solvation energy resulting from embedding the particle into the dielectric medium and will be further discussed in the next section. The term E_2 is the usual Coulomb energy between two point charges. The terms E_3, E_4, etc. are the polarization contributions, with E_3 being the leading order correction. The indices α and β represent the free charges, and the indices i, j, k etc. represent the interfaces that are consecutively polarized.

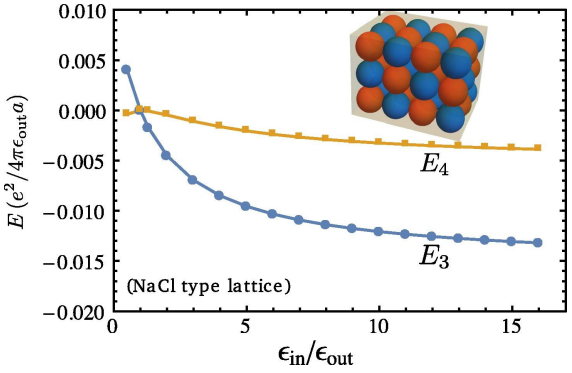

Fig. 2 The contribution to the cohesive energy of a periodic lattice of polarizable ionic aggregates due to interfacial charge polarization. The Madelung's constant[46] contains contributions from different levels of polarization interactions, E_3 and E_4 in Eq. (16), that vary with the relative permittivity of particle ϵ_{in} and medium ϵ_{out}.[27] Only results for the NaCl type lattice are shown, and similar effects are expected for other lattices. Reproduced with permission from **Fig. 4** of ref. 27.

Equation (16) is the main result of the multiple-scattering formalism. For any given configuration, it expresses the system energy as a sum of terms involving one, two, three, and an arbitrary number of particles through the Green's function. Every term transparently depends on the particle positions. The forces and torques applied on particles can be evaluated by examining the variation of energy with particle coordinates and orientation.[36,37] The approach has been applied to quantify the cohesive energy of periodic lattices of polarizable colloidal particles,[27] represented as the permittivity-dependent Madelung's constant (**Fig. 2**).[46]

The string notation introduced above has inversion symmetry, i.e., $\{\alpha;j\ldots i;\beta\} = \{\beta;i\ldots j;\alpha\}$, which in practice can be employed to reduce the numerical calculation by a factor of two. The origin to such symmetry is that the interaction between two charges mediated by intermediate surface scattering essentially solves the two-charge boundary value problem, whose solution is unique and is irrespective of which one of the two charges is source or is acted upon. Further, the higher order strings may be conveniently evaluated by noting that the strings are transitive, i.e., a string of form $\{\alpha;j\ldots klm\ldots i;\beta\}$ can be derived by joining strings $\{\alpha;j\ldots k;l\}$ and $\{l;m\ldots i;\beta\}$. The particular advantage of strings is that they are solely determined by the relative particle positions, and no explicit reference to surface charge is needed.

1.4 Solvation energy

The formalism presented above is applicable to both free charges and charges embedded inside particle inclusions. The generalized solvation energy of a given charge α is obtained by selecting the

strings with $\beta = \alpha$, which includes terms of the form

$$E_{\text{solvation}} = \frac{1}{2}\sum_{\alpha}\Big(\{\alpha;\alpha\} + \sum_{i}\{\alpha;i;\alpha\} + \sum_{j}\sum_{i}\{\alpha;ji;\alpha\} + \cdots\Big). \quad (17)$$

The term $\{\alpha;\alpha\}$ only applies to charges embedded inside a particle. It represents the interaction between charge α and the surface charge induced by itself on its own surface. The term $\{\alpha;i;\alpha\}$ can be interpreted as follows: charge α and the induced charge on its own surface induces surface charges on the surface i, which subsequently interact with the charge α. The remaining terms are similar and involve more interfaces to be polarized.

Consider a point charge Q placed at the center of a spherical particle of radius a. The lowest order solvation energy is given by the term $\{\alpha;\alpha\}$ in Eq. (17), which evaluates to

$$E_{\text{B}} = \frac{Q^2}{8\pi\epsilon_0 a}\left(\frac{1}{\epsilon_{\text{out}}} - \frac{1}{\epsilon_{\text{in}}}\right). \quad (18)$$

The result differs from the standard Born solvation energy[2] only by a term depending on the particle permittivity ϵ_{in}. The solvation energy vanishes when the permittivity mismatch vanishes. The remaining terms in Eq. (17) are the correction to the Born solvation, due to the interactions between the embedded charge and the other nearby interfaces.

1.5 Dipolar and multipolar charges

The cloud of arbitrary charge distribution can be decomposed as a sum of contributions from monopoles, dipoles, quadrupoles, etc. The above development for monopolar charges can be carried on and applied to these multipolar cases.[1] To see this, recall that a point dipole $\boldsymbol{\mu} = q\boldsymbol{d}$ can be conceived of as the limit of two monopolar charges $\pm q$ with opposite signs spatially separated by displacement $\boldsymbol{d}$, which points from the negative to the positive charge centers. Since the potential is additive, the electrostatic potential generated by a point dipole can be treated as a sum of contributions from two monopoles, $\phi(\boldsymbol{r},\boldsymbol{\mu}) = \phi(\boldsymbol{r},+q) + \phi(\boldsymbol{r},-q)$. In the limit of a point dipole, i.e. $\boldsymbol{d}\to 0$, the above sum essentially becomes a derivative, and reduces to the dot product between the dipole moment and the gradient of the potential generated by a point charge at the center of the dipole,

$$\phi(\boldsymbol{r},\boldsymbol{\mu}) = -\boldsymbol{\mu}\cdot\nabla\phi(\boldsymbol{r}). \quad (19)$$

Likewise, the energy evaluated at one dipole is given by a similar expression, $\boldsymbol{\mu}\cdot\boldsymbol{E}$, where $\boldsymbol{E}$ is the electrical field strength evaluated at the center of dipole $\boldsymbol{\mu}$. In particular, the solvation energy of a dipolar, dielectric spherical particle is given by[37]

$$E_{\text{B,dipole}} = \frac{\mu^2}{8\pi\epsilon_0 a^3}\frac{2\epsilon_{\text{out}}}{\epsilon_{\text{in}}+2\epsilon_{\text{out}}}\left(\frac{1}{\epsilon_{\text{out}}} - \frac{1}{\epsilon_{\text{in}}}\right), \quad (20)$$

which generalizes the Born solvation energy for monopolar particles, Eq. (18). In full analogy, the field generated by a quadrupole and the energy of a quadrupole inside an externally produced field, can be obtained by differentiating corresponding expressions for dipoles. The procedures are standard,[1] and the main results, including specifically the solvation energy, have been tabulated in great detail in ref. 37.

2 External field

One practically important problem is evaluating the effective medium dielectric permittivity for composite materials, such as ceramic-polymer composites. The components typically have distinct dielectric permittivities; for instance, the relative permittivity of ceramic materials is often of order 20 and that of organic materials is often less than 10, depending on polarity. The response of the composite as a whole would then depend on the intrinsic permittivities of both components and the mixing volume fractions. A standard approach for estimating the effective permittivity is to use an appropriate mixing rule, that averages the contributions of all the components. Many such mixing rules have been proposed, among which the Maxwell-Garnett rule[47,48] remains the most widely used.[49] In essence, the Maxwell-Garnett rule connects the linear combination of the component polarizability with the effective dielectric permittivity via the Clausius-Mossotti relationship.[2] The effects of inter-particle interaction have been neglected, which makes the mixing rule only applicable in the dilute regime.

The generalization of the multiple-scattering treatment needed to study the permittivity is to consider the multiple-scattering expansion in the presence of an external field. For the static dielectric permittivity, only the presence of a static field is needed. Further, within the linear response regime, considering the limit of small field strength suffices.

This step was taken in ref. 38. Although it focuses on spherical particles, the main conclusion is general, and is summarized as follows. First consider an isolated particle embedded inside a continuum dielectric medium. Applying a static field $\boldsymbol{E}_0$ polarizes the interfaces, and the surface charges can be expanded as a sum of dipoles, quadrupoles, etc. No monpolar charges can be induced because of charge neutrality. In the linear response regime, these multipoles are linear in the field $\boldsymbol{E}_0$. In particular, the dominant dipole relates to $\boldsymbol{E}_0$ by the particle's polarizability tensor $\boldsymbol{\alpha}$,

$$\boldsymbol{\mu}_E = \boldsymbol{\alpha}\cdot\boldsymbol{E}_0. \quad (21)$$

The polarizability tensor is fully specified by the shape of the particle, and by the permittivities of particle and medium. For a spherical particle, it is isotropic, reduced to the well-known scalar form, $\alpha = 4\pi a^3\epsilon_{\text{out}}(\epsilon_{\text{in}}-\epsilon_{\text{out}})/(\epsilon_{\text{in}}+2\epsilon_{\text{out}})$. It then follows that the multiple-scattering expansion for the energy of a composite can be developed by treating the particles as containing a dipole $\boldsymbol{\mu}_E$.

To develop an analogous theory for the dielectric permittivity of composite materials, an average over particle configurations is needed. This was worked out in ref. 38, whereby a virial expansion was derived for the free energy of a composite containing polarizable particles, for the average polarization in the vanishing field limit, and eventually for the effective medium dielectric permittivity. For monodisperse composites, the average medium permittivity ϵ_{m} is expressed as

$$\frac{\epsilon_{\text{m}}-\epsilon_{\text{out}}}{\epsilon_{\text{m}}+2\epsilon_{\text{out}}} = \frac{4\pi}{3}\frac{\epsilon_{\text{r}}-1}{\epsilon_{\text{r}}+2}\tilde{\rho} + B_0(\epsilon_{\text{r}})\tilde{\rho}^2 + \cdots \quad (22)$$

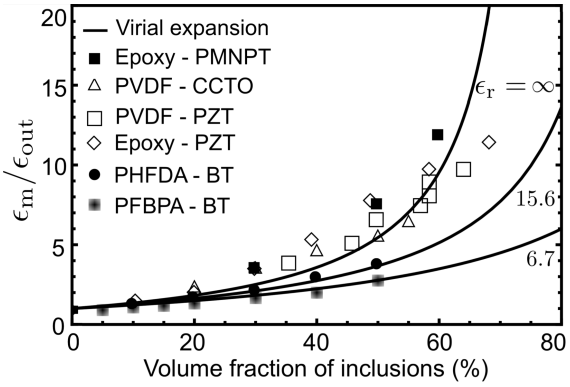

Fig. 3 Effective static dielectric permittivity for well-dispersed composites, with a range of relative dielectric permittivity between particle inclusion and medium ϵ_r. The data points are distinct experimental results measured in the static limit.[38] The solid lines are parameter-free prediction given by Eq. (22). The conducting limits are reached for large values of ϵ_r. The Maxwell-Garnett rule predicts a much weaker variation.[38] Reproduced with permission from **Fig. 5** of ref. 38.

Above $\epsilon_r \equiv \epsilon_{in}/\epsilon_{out}$ is the relative permittivity controlling the strength of the interfacial polarization, $\tilde{\rho} \equiv 4\pi a^3\rho/3$ is the volume fraction of particle inclusions, and $B_0(\epsilon_r)$ is the second dielectric virial expansion coefficient whose strength depends on the relative permittivity. This particular representation of the permittivity suggests that the effective permittivity of monodisperse composites only depends on the volume fraction, but not on particle radius, an expected result since particle radius and inter-particle separation are the only two physical lengths in the problem.

Terminating the expansion at the term linear in $\tilde{\rho}$ gives a result identical to the Maxwell-Garnett expansion.[47–49] Including the second order term requires evaluating the virial coefficient $B_0(\epsilon_r)$ numerically. The explicit values of B_0 have been tabulated in ref. 38 over the entire range of relative dielectric permittivity. It reaches the limiting value $56\pi^2/81$ for conducting inclusions, i.e. as $\epsilon_r \to \infty$, and reaches $-8\pi^2/81$ for the opposite limit with $\epsilon_r \to 0$, which is realized in porous materials with very high medium permittivity. The comparison of the predicted permittivity using Eq. (22) with experimental values over a wide range of dielectric permittivity shows that much of the nonlinear dependence on particle fraction is captured by the second order dielectric virial expansion, with no adjustable parameters (**Fig. 3**).

3 Surface Green's function

The multiple-scattering expansion provides a formal solution to Poisson's equation with sharp dielectric interfaces. It is supported by the linearity of Poisson's equation. The essential step needed to make quantitative predictions is the evaluation of the single particle Green's function, which gives the electrostatic potential produced by a point charge near the scattering interface. The Green's function, in practice, is typically evaluated numerically and tabulated. The transparent solutions for a handful of examples are well-known. For a flat interface separating two bulk dielectric domains, it is given by the standard image charge construction.[1] For a flat slab confined by two half-space dielectric domains, it is given by more elaborate expressions.[12,50] For a conducting sphere, it is also given by the image charge which is introduced to ensure that the conducting surface is equipotential.[1]

For a spherical dielectric interface, the Green's function has been discovered[39] and re-discovered many times.[33,36,40–42] It was found that the image charge approach still applies. The Green's function $\tilde{g}$, representing the electrostatic potential at a spatial position $\boldsymbol{r}$ generated by the surface charge induced by a given source charge Q_0 placed at $\boldsymbol{R}_0$ (**Fig. 1**), can be written

$$\tilde{g}(\boldsymbol{r};\boldsymbol{R}_0,Q_0) = \frac{Q_0'}{4\pi\epsilon_0\epsilon_{out}}\left(\delta_{s,1} - g\int_0^1 \mathrm{d}s\, s^{g-1}\right)\frac{1}{|\boldsymbol{r} - s(a^2/R_0)\hat{\boldsymbol{R}}_0|}, \tag{23}$$

where $Q_0' \equiv Q_0\frac{\epsilon_{out}-\epsilon_{in}}{\epsilon_{out}+\epsilon_{in}}\frac{a}{R_0}$ is the strength of the image charge, $R_0 = |\boldsymbol{R}_0|$ is the distance of the source charge to the center of the sphere, $\hat{\boldsymbol{R}}_0 = \boldsymbol{R}_0/R_0$ is the normal vector, and $g \equiv \epsilon_{out}/(\epsilon_{in}+\epsilon_{out})$ determines the image charge distribution. It has been shown[36] that Eq. (23) satisfies the boundary condition Eq. (1), thus uniquely determines the static potential generated by the polarized spherical surface.

The contribution from the first term in the bracket can be understood as resulting from placing an image charge Q_0' at the Kelvin point,[1] $(a^2/R_0)\hat{\boldsymbol{R}}_0$. In the conducting limit ($\epsilon_{in} \to \infty$) it reduces to the known value $-(a/R_0)Q_0$.[1] The contribution from the second term in the bracket can be understood as resulting from the potential generated by a line charges: the line extends from the center of the sphere to the Kelvin point, and the charge density at the fractional distance s to the center is gs^{g-1}. This image line, known as the Neumann line,[39,40] complements the Kelvin image point and solves the Poisson's equation with the spherical boundary. Eq. (23) effectively replaces the effect of the two-dimensional surface charges with that of a one-dimensional line charge, which reduces computational costs in practice.

The strength of the surface polarization depends on the particle radius a and the distances of the source (R_0) and the field (r) to the center of the sphere. Expanding the last term in Eq. (23) in terms of the powers of s shows that the contribution from the term of order s^0 vanishes, and that from the term of order s^1 gives the leading contribution

$$\tilde{g}(\boldsymbol{r};\boldsymbol{R}_0,Q_0) \simeq -\frac{Q_0}{4\pi\epsilon_{out}}\left(a^3\frac{\epsilon_{in}-\epsilon_{out}}{\epsilon_{in}+2\epsilon_{out}}\right)\frac{\boldsymbol{R}_0\cdot\boldsymbol{r}}{R_0^3 r^3}. \tag{24}$$

Therefore, the strength of the static potential produced by a single polarized sphere is determined by the product between the polarizability of the sphere, $a^3(\epsilon_{in}-\epsilon_{out})/(\epsilon_{in}+2\epsilon_{out})$, and $(R_0 r)^{-2}$. In the typical case, when both R_0 and r are of the order of the average inter-particle separation d, Eq. (24) is smaller than the non-polarized Coulombic potential, $Q_0/(\epsilon_{out}d)$, by a factor $(a/d)^3$.

The Green's function $\tilde{g}_i \circ \tilde{g}_i$ for the string of type $\{\boldsymbol{r}; ji; 0\}$ is obtained by propagating the Kelvin image point and Neumann image line.[36] One first finds the primary image of source charge Q_0 in the sphere i, then finds the images of the primary image in the sphere j, which finally acts at the position $\boldsymbol{r}$. The final result[36] reads

$$\tilde{g}_j \circ \tilde{g}_i = \frac{Q_0}{4\pi\epsilon_0\epsilon_{out}\sqrt{R_{43}R_{21}}}\mathscr{I}_j\mathscr{I}_i\frac{1}{|f_i\hat{\boldsymbol{R}}_{21} + \hat{\boldsymbol{R}}_{32} + f_j\hat{\boldsymbol{R}}_{43}|}, \tag{25}$$

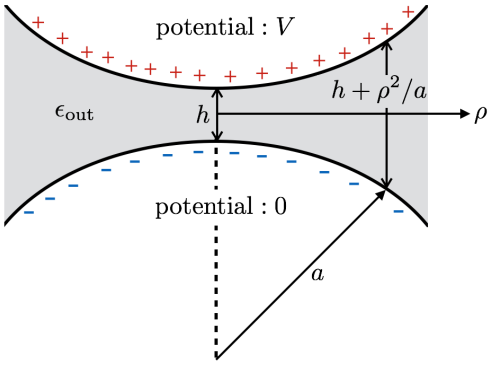

Fig. 4 Contact charges between two conducting spheres approaching each other. The two conducting spheres are equipotential, and the potential values are set as V and 0. The charge distributions are adapted to produce the nearly vertical field lines, The gap distance is h, and the separation for non-vanishing radial distance ρ is $h+\rho^2/a$ for small gap distance, according to the Derjaguin approximation.[2]

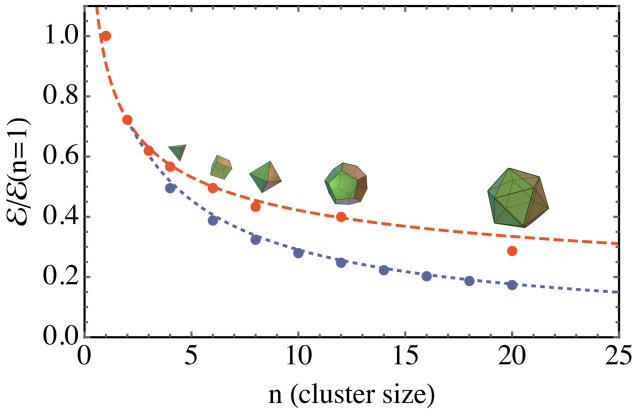

Fig. 5 Cohesive energy of lower order clusters composed of identical conducting spheres in contact. The contribution from the singular contact charges has been fully accounted for. Upper curve: $(2/n)^{1/3}/(2\ln 2)$, the continuum limit for the energy of most compact configuration. Lower curve: $\ln(2na/r_0)/[n\ln 2\ln(2a/r_0)]$, the energy of a conducting cylinder with an identical volume, i.e., with length $L=2na$ and radius $r_0=0.816a$.[52] Reproduced with permission from **Fig. 5** of ref. 52.

where $\boldsymbol{R}_{43}\equiv\boldsymbol{r}-\boldsymbol{R}_j$, $\boldsymbol{R}_{32}\equiv\boldsymbol{R}_j-\boldsymbol{R}_i$, $\boldsymbol{R}_{21}\equiv\boldsymbol{R}_i-\boldsymbol{R}_0$, and $\boldsymbol{R}_j$ and $\boldsymbol{R}_i$ are the positions of the centers of the spheres j and i. The summation over images, denoted by $\mathscr{I}_i$ and $\mathscr{I}_j$, are defined by

$$\mathscr{I}_k\equiv\frac{\epsilon_{\rm out}-\epsilon_{\rm in}}{\epsilon_{\rm out}+\epsilon_{\rm in}}\,t_k\left(\delta_{f_k,t_k^2}-g\,t_k^{-2g}\int_0^{t_k^2}{\rm d}f_k\,f_k^{g-1}\right)$$

with $k=i$ or j, $t_j\equiv a/\sqrt{R_{43}R_{32}}$, and $t_i\equiv a/\sqrt{R_{32}R_{21}}$. A Taylor expansion analogous to the above shows that Eq. (25) is of order $(a/d)^6$ compared to the direct Coulomb interaction. This scaling is generic: the transparent expressions for image lines needed to evaluate a string of n intermediate interfacial polarization are provided in ref. 36, and their orders of magnitude are smaller than the direct Coulomb interaction by a factor $(a/d)^{3n}$.

The above result the Green's function is applicable to spherical particles. A Green's function has also been discovered for anisotropic nematic dielectric domains with planar interfaces,[51] by absorbing the dielectric profile into the coordinate transformation. The extension of this approach to spherical domains, or with a more complicated permittivity tensor, is still to be worked out.

4 Contact singularity

Interfacial polarization is particularly relevant at small interparticle separation. Thus for practical applications involving dilute suspensions, the effects of induced surface charges can be evaluated with the multiple-scattering series truncated at lower orders. However, the polarization does strengthen with reduced separation, which can cause practical difficulties for cases involving particles forming close contact. In certain cases, the contact charging effects become singular; evaluating the energy would be plagued by numerical divergence, stymieing the practical application of the series expansion.[31,32]

To reveal the contact singularity, it is instructive to examine the contact formed between two approaching, conductive surfaces, for which the interfacial polarization is the strongest. Consider two spherical conducting particles. Let one of them, say sphere 1, carry a source charge q_1. The source charge induces surface charges on sphere 2, which subsequently induces surface charges on sphere 1. This recursive reflection continues indefinitely. The smaller the gap width between the two approaching surfaces, the greater number of reflective terms required to ensure convergence. Right at the contact, an infinite number of such reflective terms are needed, which translates to diverging image charges of opposite signs of the two surfaces.

The magnitude of the diverging charge for one of the two conductors in contact is of order $\pi\epsilon_{\rm out}a\ln(a/h)$,[52] where h is the gap distance between the two spheres, and a is the sphere radius. This divergent contact charge is needed to establish the potential difference near the gap and may be obtained by considering the vicinity of two spheres near contact depicted in **Fig. 4**. Since the conducting spheres are equipotential, the static potentials everywhere on the surfaces are identical. Denote their difference as V. For small separation h, the Derjaguin approximation[2] can be applied to represent the two surface as parabolic. Denote further the radial length by ρ, the distance separating the two spheres can be written as $h+\rho^2/a$, which is asymptotically exact for $h\to 0$. The field strength at radius ρ is $E(\rho)=V/(h+\rho^2/a)$, which is $1/\epsilon_{\rm out}$ times of the induced charge density (note that the electric field inside a conductor vanishes, so there is no contribution from $\epsilon_{\rm in}$).[1] Integrating ρ from 0 to ca, in which c is an order unit numerical cutoff to ensure the validity of the Derjaguin approximation,[2] gives the singular portion of the induced charge

$$Q_{\rm singular}=\int_0^{ca}{\rm d}\rho\,\frac{2\pi\rho\,\epsilon_{\rm out}V}{h+\rho^2/a}=\pi\epsilon_{\rm out}\,aV\ln(a/h)\,,\qquad(26)$$

in which the non-singular factor $\ln(c^2)$ has been dropped. This contact charge can also be obtained using the multiple-scattering formalism when only two conducting spheres are considered.[53,54] In that approach, one image charge is introduced for one interfacial scattering.[55] For vanishing gap separation h, an infinite number of image charges or interfacial scatterings are required, which ultimately expresses the induced surface charges in terms of an infinite series. Pulling out the asymptotic, diverging

contact charge from such a series gives an expression identical to that from the analysis based on the Derjaguin approximation. The Derjaguin approximation, relying on geometric properties near the contact, however can be applied to the case of *multiple* conducting particles in close contact.

Eq. (26) clearly shows that the singular capacitance Q/V diverges logarithmically as $h \to 0$. For any finite potential difference between the spheres, resolving the induced surface charges at small separation requires ever increasing spatial resolutions as h decreases. The practical calculation of the surface charges at small separation would need to numerically remove the contribution from this singular capacitance.

The case of two spheres of unequal radii in close contact has been analyzed by Russell,[53] and the singular portion of the charge density is obtained by replacing the sphere radius with the harmonic mean of the two radii, $2a_1a_2/(a_1+a_2)$. Because the contact singularity is local, the same behavior is expected for contacts formed between conducting particles of arbitrary shape, being convex or concave. In these cases, the sphere radii are replaced by the radii of curvature near the contacts.

The singular capacitance imposes a steep separation dependence of interaction energy between polarizable spheres.[52] As a result, the cohesive energy between two particles, identified as the difference of the interaction energy at contact or at an infinite separation, is strongly affected by this effect. In the case of dimers, the cohesive energy was found to be[56]

$$\frac{1}{4\pi\epsilon_{\rm out}a}\frac{(Q_1+Q_2)^2}{2\ln 2}, \tag{27}$$

where Q_1 and Q_2 are the net charges on the two spheres.

The ensemble of multiple polarizable conducting spheres has no analytically closed-form solution, but can be evaluated numerically by isolating the contribution of singular capacitance.[52] The method has been applied to ensembles of up to 20 identical spheres. Two types of particle packings are considered. The first type is more compact, which places the spheres at the vertices of Platonic solids including tedrahedron, cubic, octahedron, dodecahedron, and icosahedron (**Fig. 5**). The second type is the most open, which places the spheres along a straight line. Charging one sphere in these clusters with an elementary charge (it does not matter which one is charged when all the spheres are in contact because the whole cluster becomes equipotential), and calculating the total electrostatic energy gives the cohesive energy for these clusters. The cohesive energies are dominated by the contact charge, and are plotted in **Fig. 5**, for both *compact* and *open* configurations. It was found that the cohesive energies of both compact and open configurations can be understood by treating the clusters in close contact as equipotential. The compact clusters can be approximated (geometrically) as spherical capacitors whose radius is determined from the size of the cluster. Likewise, the open clusters can be approximated as cylindrical capacitors whose length is the same as the number of spheres times their diameter and whose radius is calculated by equating the volume of the cylindrical capacitor and that of the cluster. The dashed lines in **Fig. 5** are the energies of the spherical and cylindrical capacitors with identical volume, which approximately the numerically evaluated cohesive energy of these clusters remarkably well.

A similar type of contact singularity is expected for dielectric spheres. This is clearly seen from the numerical examples provided in the literature.[31,32] An analytical treatment similar to that of ref. 52 but relying on the application of bispherical coordinates was developed recently,[38] albeit only for dimer spheres carrying identical charges. The resulting cohesive energy depends explicitly on the dielectric permittivity of spheres, and reduces to Eq. (27) in the conductor limit, i.e. $\epsilon_{\rm in} \to \infty$. The asymmetric case, with $Q_2 \neq Q_1$, remains to be tackled.

5 Summary and outlook

The multiple-scattering formalism is an iterative, flexible framework for solving boundary value problems. Since the governing equation, e.g., Poisson's equation, is additive, the solution can be constructed iteratively. The components to be iterated are the Green's functions for single, isolated boundaries. This formalism, in principle, also applies to transport phenomena in the low-Reynolds number regime, in which the Stokes equation and the velocity profile play the role of the Poisson equation and the electrostatic potential, respectively.[43] The dielectric permittivity likewise plays the role of viscosity. Thus there is a close analogy between the problems of polarization and low-Reynolds number hydrodynamics.[44] Much of the issues touched upon here, including the contact singularity and the Green's function, have been addressed in the context of hydrodynamics.[57]

Polarization is weak compared to the direct Coulombic interaction. Its strength is controlled by the relative dielectric permittivity at the interface and by the polarizability of particles as is clearly revealed by Eqs. (23–24). The scaling behaviors of the terms needed to evaluate the terms in the multiple-scattering series have been discussed based on the consideration of the leading term, Eq. (24).[36] Qualitatively, every additional interfacial scattering reduces the numerical value of the string by a factor proportional to the polarizability of particles. Since the polarizability scales as the volume of particle a^3, the strength of polarization effect scales, according to Eq. (24), as ρa^3, where the particle number density ρ is used to estimate the average inter-particle separation, $R_0 \sim \rho^{-1/3}$.[36] In cases involving short inter-particle separations, and strong dielectric discontinuities, the polarization has been demonstrated to alter the qualitative behavior of the interaction among particles. The like-charge attraction and non-additive many-body interaction potential derived by the surface polarization are two well-known examples.[25–27,30]

In practice, the number of terms to evaluate grows rapidly with the number of particles,[36] although imposing the symmetry of strings can simplify the calculation to certain degree. Thus, the method reviewed here is useful primarily for aggregates involving lower-order clusters, and for systems with sharp, yet weak dielectric discontinuities, where the polarization effects are local. Systems involving spatially varying dielectric permittivity will require, in essence, inverting dense coefficient arrays, which makes the alternative variational approach more attractive.[35] The main advantage of the multiple-scattering formalism is that every term in the series bears a simple physical interpretation.

Many questions can be addressed using the formalism developed here. The dielectric virial expansion developed only applies to spherical particles, and for static permittivity. It would be desirable to generalize the theory to systems with anisotropic particle inclusions (i.e., keeping the tensorial form of polarizability and tracking the orientational degrees of freedom), and with polydisperse inclusions (i.e., performing statistical averages for a mix of different particle types). Another extension is to develop an analogous theory for the frequency-dependence of the effective medium permittivity, which demands a treatment analogous to those in the Lifshitz theory for the Van der Waals interaction.[2,58] Furthermore, by replacing the internal dielectric permittivity of the particles with the molecular polarizability using the Clausius-Mossotti relation,[2] it is possible to investigate the effects of ion polarizability on various electrochemical phenomena including, specifically, the effects of ion polarizability on surface tension. The standard DLVO theory[2] for the effective potential between colloidal particles is also expected to be affected by the interfacial charge polarization, and should be studied in the future.

Conflicts of interest

There are no conflicts to declare.

Acknowledgements

This research has been supported by the Assistant Secretary for Energy Efficiency and Renewable Energy, Office of Vehicle Technologies of the U.S. Department of Energy through the Advanced Battery Materials Research (BMR) Program (Battery500 Consortium). The supports provided through the Terman Faculty Fund, the 3M Non-Tenured Faculty Award, and the Hellman Scholar Award are acknowledged. The author thanks Prof. Karl Freed gratefully for discussions throughout, and Huada Lian and Kevin Hou for critical reading of the manuscript.

References

1 J. D. Jackson, *Classical Electrodynamics*, Wiley, 3rd edn, 1998.
2 J. N. Israelachvili, *Intermolecular and Surface Forces*, Academic Press, New York, 1992.
3 K.-D. Kreuer, *Chem. Mater.*, 2013, **26**, 361–380.
4 E. Gouaux and R. MacKinnon, *Science*, 2005, **310**, 1461–1465.
5 E. V. Shevchenko, D. V. Talapin, N. A. Kotov, S. O'brien and C. B. Murray, *Nature*, 2006, **439**, 55.
6 S. R. Waitukaitis, V. Lee, J. M. Pierson, S. L. Forman and H. M. Jaeger, *Phys. Rev. Lett.*, 2014, **112**, 218001.
7 V. Lee, S. R. Waitukaitis, M. Z. Miskin and H. M. Jaeger, *Nature Physics*, 2015, **11**, 733–737.
8 M. E. Leunissen, A. Van Blaaderen, A. D. Hollingsworth, M. T. Sullivan and P. M. Chaikin, *Proc. Natl. Acad. Sci.*, 2007, **104**, 2585–2590.
9 I. N. Derbenev, A. V. Filippov, A. J. Stace and E. Besley, *J. Chem. Phys.*, 2016, **145**, 084103.
10 R. Messina, *J. Chem. Phys.*, 2002, **117**, 11062.
11 A. Bakhshandeh, A. P. Dos Santos and Y. Levin, *Phys. Rev. Lett.*, 2011, **107**, 107801.
12 J. W. Zwanikken and M. Olvera de la Cruz, *Proc. Natl. Acad. Sci.*, 2013, 201302406.
13 H. S. Antila and E. Luijten, *Phys. Rev. Lett.*, 2018, **120**, 135501.
14 H. Gong and K. F. Freed, *Phys. Rev. Lett.*, 2009, **102**, 057603.
15 A. Abrashkin, D. Andelman and H. Orland, *Phys. Rev. Lett.*, 2007, **99**, 077801.
16 L. Onsager and N. N. Samaras, *J. Chem. Phys.*, 1934, **2**, 528–536.
17 M. Boström, W. Kunz and B. W. Ninham, *Langmuir*, 2005, **21**, 2619–2623.
18 I. Langmuir, *J. Am. Chem. Soc.*, 1917, **39**, 1848–1906.
19 C. Wagner, *Phys. Z*, 1924, **25**, 474–477.
20 N. L. Jarvis and M. A. Scheiman, *J. Phys. Chem.*, 1968, **72**, 74–78.
21 E. Knipping, M. Lakin, K. Foster, P. Jungwirth, D. Tobias, R. Gerber, D. Dabdub and B. Finlayson-Pitts, *Science*, 2000, **288**, 301–306.
22 S. Ghosal, J. C. Hemminger, H. Bluhm, B. S. Mun, E. L. Hebenstreit, G. Ketteler, D. F. Ogletree, F. G. Requejo and M. Salmeron, *Science*, 2005, **307**, 563–566.
23 Y. Levin, *Phys. Rev. Lett.*, 2009, **102**, 147803.
24 A. P. dos Santos, A. Diehl and Y. Levin, *Langmuir*, 2010, **26**, 10778–10783.
25 E. Bichoutskaia, A. L. Boatwright, A. Khachatourian and A. J. Stace, *J. Chem. Phys.*, 2010, **133**, 024105.
26 E. B. Lindgren, H.-K. Chan, A. J. Stace and E. Besley, *Phys. Chem. Chem. Phys.*, 2012, **18**, 5883–5895.
27 J. Qin, J. Li, V. Lee, H. Jager, J. J. de Pablo and K. F. Freed, *J. Colloid Interface Sci.*, 2016, **469**, 237 – 241.
28 J. C. Crocker and D. G. Grier, *Phys. Rev. Lett.*, 1996, **77**, 1897–1900.
29 S. K. Sainis, J. W. Merrill and E. R. Dufresne, *Langmuir*, 2008, **24**, 13334–13337.
30 J. W. Merrill, S. K. Sainis and E. R. Dufresne, *Phys. Rev. Lett.*, 2009, **103**, 138301.
31 K. Barros and E. Luijten, *Phys. Rev. Lett.*, 2014, **113**, 1–5.
32 K. Barros, D. Sinkovits and E. Luijten, *J. Chem. Phys.*, 2014, **140**, 64903.
33 Z. Gan, S. Jiang, E. Luijten and Z. Xu, *SIAM J. Sci. Comput.*, 2016, **38**, 375–395.
34 X. Jiang, J. Li, X. Zhao, J. Qin, D. Karpeev, J. Hernandez-Ortiz, J. J. de Pablo and O. Heinonen, *J. Chem. Phys.*, 2016, **064307**, year.
35 V. Jadhao, F. J. Solis and M. Olvera de la Cruz, *J. Chem. Phys.*, 2013, **138**, 054119.
36 J. Qin, J. J. de Pablo and K. F. Freed, *J. Chem. Phys.*, 2016, **145**, 124903.
37 K. S. Gustafson, G. Xu, K. F. Freed and J. Qin, *J. Chem. Phys.*, 2017, **147**, 064908.
38 H. Lian, J. Qin and K. F. Freed, *J. Chem. Phys.*, 2018, **149**, 163332.
39 C. Neumann, *Hydrodynamische Untersuchen nebst einem An-*

hang uber die Probleme der Elecktrostatik und der Magnetischen Induktion, Teubner, Leipzig, 1883, pp. 279–282.
40 I. V. Lindell, *Am. J. Phys.*, 1993, **61**, 39–44.
41 W. Cai, S. Deng and D. Jacobs, *J. Comp. Phys.*, 2007, **223**, 846.
42 P. Linse, *J. Chem. Phys.*, 2008, **128**, 214505.
43 D. J. Jeffrey and A. Acrivos, *AIChE J.*, 1976, **22**, 417–432.
44 J. Happel and H. Brenner, *Low Reynolds number hydrodynamics: with special applications to particulate media*, Martinus Nijhoff Publishers, 1983.
45 T. P. Doerr and Y.-K. Yu, *Phys. Rev. E*, 2006, **73**, 061902.
46 N. W. Ashcrof and N. D. Mermin, *Solid State Physics*, Thomson Learning, Inc., 1976.
47 J. C. Maxwell Garnett, *Phil. Trans. Royal Soc. A*, 1904, **203**, 385–420.
48 L. Rayleigh, *Phil. Mag.*, 1892, **34**, 481–502.
49 V. A. Markel, *J. Opt. Soc. Am. A*, 2016, **33**, 1244–1256.
50 R. Kjellander and S. Marčelja, *J. Chem. Phys.*, 1985, **82**, 2122–2135.
51 E. J. Mele, *Am. J. Phys.*, 2001, **69**, 557–562.
52 J. Qin, N. W. Krapf and T. A. Witten, *Phys. Rev. E*, 2016, **93**, 022603.
53 A. Russell, *Proc. Phys. Soc. London*, 1922, **35**, 10–29.
54 J. Lekner, *Proc. Royl. Soc. A*, 2012, **468**, 2829–2848.
55 W. R. Smythe, *Static and Dynamic Electricity*, Taylor & Francis, 3rd edn, 1989.
56 J. C. Maxwell, *Proc. Math. Soc. London*, 1878, **IX**, 94–101.
57 S. Kim and S. J. Karilla, *Microhydrodynamics: Principles and Selected Applications*, Butterworth-Heinemann, Boston, 1991.
58 Y. S. Barash and V. L. Ginzburg, *Sov. Phys. Usp.*, 1984, **27**, 467–491.

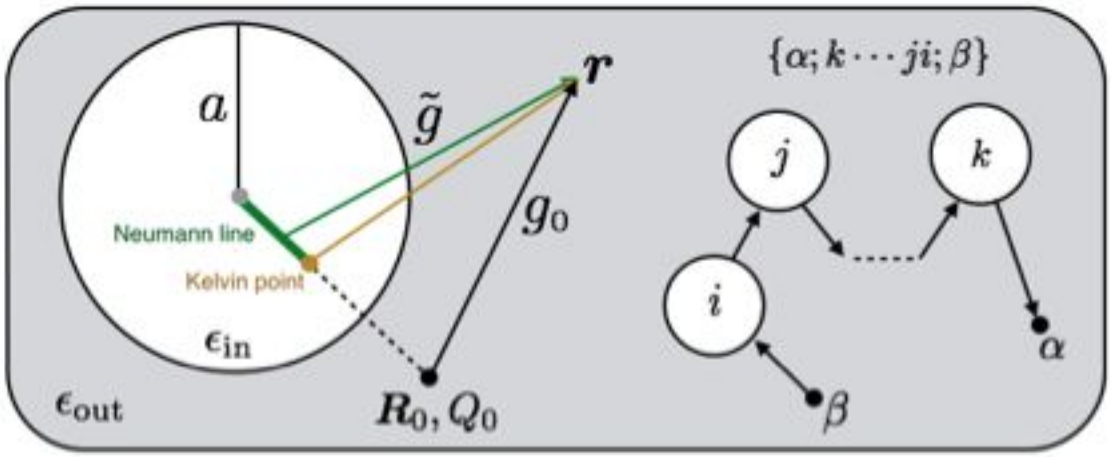

Reviewing the impacts of interfacial charges on the cohesive energy, permittivity, and singular contact charge for polarizable dielectric particles.